

# Understanding Flame Spread Across Alcohol Pools

Howard D. Ross  
Microgravity Combustion Science Branch/ MS 500-115  
Microgravity Science Division  
NASA Glenn Research Center  
Cleveland, OH 44135-1062

Fletcher J. Miller  
National Center for Microgravity Research for Fluids and Combustion / MS 110-3  
NASA Glenn Research Center  
Cleveland, OH 44135-3191

## ABSTRACT

Findings from recent experiments on flame spread across pure alcohol pools are presented with an emphasis on the effects of buoyancy, opposed forced airflow, and pool size. Predictions and/or experiments show gravity affects the spread rate at all initial pool temperatures, whether above or below the flash point. Pool dimensions also have a strong influence on both spread rate and spread behavior. At superflash temperatures, faster spread is found in microgravity ( $\mu\text{g}$ ). At low pool temperatures, forced airflow is needed to sustain flame spread in  $\mu\text{g}$ , while in 1g the flame sustains itself in a pulsating mode. As predicted, but not observed previously, experiments with shallow pools in an opposed airflow show pulsating spread in  $\mu\text{g}$ . Despite predictions of its existence, however, pulsating spread in  $\mu\text{g}$  with deep pools is not yet observed. Hypothesized causes of this disagreement and of pulsating spread in general are examined.

**KEYWORDS:** Fire, Flame Spread, Microgravity, Liquid Fuels, Alcohols, Combustion

## INTRODUCTION

The accidental ignition and flame spread across pools of flammable liquids are practical concerns in residential, commercial, and industrial settings, and particularly in aircraft work sites and crashes. Most research in this area has focussed on alcohols because of their well-known thermophysical properties and their use in chemical purification and processing. From a research perspective, the subject is rich with surprises and challenges because of the

complicated fluid mechanics and heat transfer processes that must be measured or predicted in order to interpret flame spread behavior.

Flame spread across liquid fuels differs from solids in many ways. Most important among these, liquid motion increases the flame spread rate and there is significant, flame-driven flow in both gas and liquid phases when the pool temperature,  $T_o$ , is below the fuel's flash point temperature,  $T_{FL}$ . There is also coupling between buoyancy forces and thermocapillary forces in driving the liquid motion. Characteristic regimes of flame spread across liquids are identified in **fig. 1**, with three below  $T_{FL}$ , labeled 'pseudo-uniform, pulsating, and uniform', and two above labeled 'superflash-lean and superflash-maximum'.

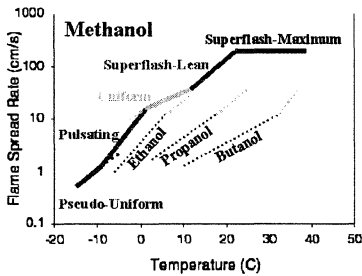


**FIGURE 1** Methanol flame regimes with other alcohol behavior in pulsating and uniform regime shown qualitatively, based on [8].

The principal goal of recent research is the detailed identification of the mechanisms that control the rate and nature of flame spread in each of these regimes. Unfortunately, disagreements persist on experimental observation of flame spread phenomenology, subsequent interpretation [1-4], and especially on the role of gravity in each of these regimes. In general, experiments have outpaced prediction, so models are used most often *a posteriori* as interpretive aids of experimental findings. State-of-the-art models do not yet include all of the potentially important processes, and this renders uncertain the ability to anticipate observations when new initial

conditions are used in experiments. For example, one cannot easily predict the flow and flame behaviors in a pool that is wider and deeper than one used in earlier experiments. Until recently there was no ability to predict, even qualitatively, what would happen if gravitational influence was eliminated. It was unknown whether ignition delay times would increase or decrease, whether flame spread would be sustained in microgravity ( $\mu g$ ) and if so, whether the spread of the flame would be faster or slower, or finally what the flame spread character would be. Thus, key questions remain, and are discussed in this review, where we specialize the subject to highlight the roles of a few of the gravity-related processes and the effects of pool dimensions (especially width and depth).

Gravity affects ignition and flame spread of liquid fuel pools in the following ways: (a) equilibrium shape of the liquid's free surface prior to the application of spot heating by an igniter or flame; (b) deformed shape of the liquid's free surface during application of spot heating; (c) wave amplitude and damping; (d) pre-ignition stratification of more dense liquid below less dense liquid; (e) pre-ignition stratification of more dense gases below less dense gases (e.g. fuel vapor distribution) (f) hydrostatic pressure in the liquid and the gas phases; (g) pre-ignition, evaporative-buoyant convection in either phase; (h) buoyant convection during spread in the liquid phase; and (i) buoyant convection during spread in the gas phase. All of the gravity-related effects are summarized in [5] whereas herein we focus only on buoyant convection. Toward resolving the effects of buoyancy on this flame spread problem, comparisons – between 1g and  $\mu g$  experimental observations, and between model predictions and experimental data at each of these gravitational levels – are extensively utilized. A

complete review of the field is included in [2], and this article provides a review of progress since that time.

## SUPERFLASH SPREAD

Flame propagation through *non-uniform* premixed gas systems (also called “layered systems”), as occurs for liquid above  $T_{FL}$ , has been the subject of relatively few previous studies. Typical experiments involve a temperature-controlled pool that is physically isolated from the air by a sealed cover plate. The plate is then removed and fuel vapor diffuses into

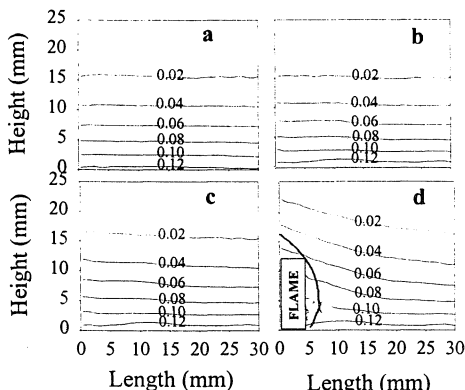


**FIGURE 2** Isoconcentration lines above a methanol pool. (a) initial fuel concentration in mole fraction; (b) 0.033 s before flame arrives; (c) 0.016 s before flame arrives; (d) flame arrival [11].

the air prior to ignition. The flame spread rate is affected strongly by the distribution of the fuel vapor above the pool at the time of ignition. The main parameters governing this distribution are the diffusion time, the temperature of the pool (which controls the vapor pressure at the pool surface), and any gas-phase flow that may be externally imposed or naturally generated due to buoyancy during the evaporation process [2].

Behavior and appearance of the flame also depend on whether  $T_O$  is high enough to create a stoichiometric concentration of fuel vapor and air. For  $T_O < T_{ST}$  ( $T_{ST}$  is the temperature at which a

stoichiometric mixture exists at the surface), the presence of the pool affects the flame spread rate even though a flammable gas-phase mixture exists prior to ignition. The spread rate for sub-stoichiometric conditions has an exponential dependence on temperature when the diffusion time is held constant and short[6]. For  $T_O > T_{ST}$ , a triple flame exists [7] and the spread rate reaches and maintains a maximum value, independent of  $T_O$  (cf. fig. 1) [8]. Flame spread is enhanced by gas-phase motion ahead of and in the same direction as spread [9a, 10]. The motion is driven by the expansion of the low-density products, which displaces and redistributes the unburned gas layers ahead of the flame into a broader, curved area (fig. 2). As the flame approaches, the iso-concentration lines are displaced upwards, and the height of the lean-limit layer is shifted[6, 11]. The flame burns in regions both below and above this height as it spreads, indicating that a flame is sustained below the lean limit (0.067 for methanol, based on  $T_O$ ), if it is burning in proximity to a region with more fuel vapor.

The effects of initial pool temperature and gravity were examined recently by simulating ignition and flame spread across propanol-air mixtures in the superflash regime at 1g and  $\mu g$  [12]. Propanol in axisymmetric, shallow pools was selected because of previous agreement between model and experiments in subflash pools [13]. A range of superflash pool temperatures was simulated (see fig. 3). As expected, independent of gravity level, spread is more rapid at higher  $T_O$  and it is steady, consistent with experiments. Interestingly, flame

spread is predicted to be more rapid in  $\mu g$  than in  $1g$ [12]; this is in opposition to a stream-tube model developed for this problem, which did not consider buoyancy, that predicted higher velocities at  $1g$  due to a hydrostatic pressure effect[9b]. The speed of the flame spread is predicted now to be slightly faster in microgravity for two reasons. First, thermal expansion behind the flame front in the uniform spread regime strongly drives the flame forward. In  $1g$ , buoyancy in the trailing portion of the flame carries some of this thermal expansion upward and away from the flame front. Additionally, buoyant airflow toward the flame opposes the direction of flame spread. Both of these effects are absent in microgravity, thus the flame is predicted to spread faster in microgravity. Experimentally, in a long gallery the  $\mu g$  flame appears to spread faster for the same diffusion time, though this must be considered a preliminary result, as more data are required to verify this trend[12]. The predicted effect of gravity diminishes as  $T_O$  increases, as was hypothesized [6].

### UNIFORM FLAME SPREAD

The regime of uniform flame spread is defined by the range of  $T_O$  just below  $T_{FL}$  that supports a flame that spreads across the fuel pool at a steady rate. The range has been catalogued experimentally for flame spread across light alcohol fuels (through butanol) contained in narrow, long trays[8, 14]. Some of these experiments, and subsequent ones [3, 15] are now acknowledged to be influenced by the pool dimensions. For example, flames can spread uniformly across a deep pool, but pulsate across a shallow pool[16], due to heat and momentum loss to the tray bottom. Sidewalls similarly can inhibit the surface velocity and change the rate and character of spread [2], and change the spread process into a three-dimensional phenomenon.<sup>a</sup> The criticality of the pool dimensions on flame spread phenomena remains underappreciated.

The conflicting explanations of the detailed phenomenology and controlling mechanisms for uniform spread are discussed in[3]. It was

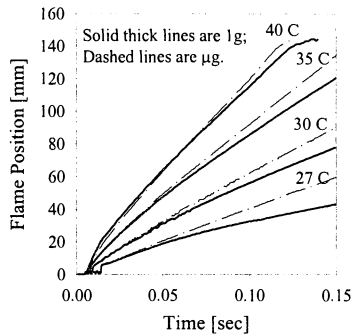


**FIGURE 3** Predicted spread across superflash propane-air pools 1.6 mm deep and 15 cm diameter.

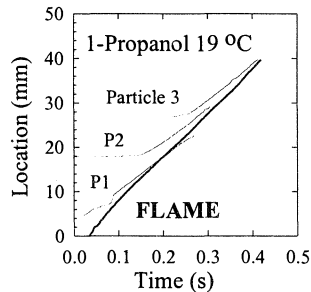


**FIGURE 4** Position of flame and 3 particles on pool surface, [3]

in a general the effects of pool dimensions diminish when  $T_O \rightarrow T_{FL}$ . So, it is in this and the superflash regime, that two-dimensional models are most applicable and most successful.

later thought that liquid-phase convection controls the uniform spread rate, at least for 0.5 cm wide pools [15]. In wider pools [3] observed through particle image velocimetry (PIV) and rainbow schlieren deflectometry (RSD), it is seen that (1) preheating is confined to a very thin (sub-mm) surface layer (based on the RSD images); and (2) as the flame approaches the surface particles in PIV tests, the particles begin moving in the same direction as the flame, but are overtaken by it (see Particle 1, **fig. 4**). The liquid convection is confined to a very thin, surface layer and, since it is overtaken by the flame, convection cannot be the only preheating mechanism (in flame-fixed coordinates, the flow is toward the flame). Thus, a second mechanism such as gas-phase conduction must be playing a role in this scale experiment.

Axisymmetric pools (1.6 mm deep, 15 cm diameter) were utilized in the first  $\mu\text{g}$  experiments [16, 17] in the temperature range associated with uniform spread. Regardless of the ambient environment ( $\text{O}_2$  concentration and diluent type were varied), for conditions where the corresponding 1g flame spread was uniform, the  $\mu\text{g}$  spread was also uniform at a rate that was similar to the 1g flame. At the time, the authors believed that the shallow pools eliminated the possibility of buoyantly driven liquid flow even in the 1g experiments, but this conclusion was incorrect because the thermal boundary layer in the liquid is smaller than the pool depth.

The above experiments and those from 1g experiments of flame spread across rectangular trays [18] were recently simulated with a state-of-the-art numerical model [19] that is transient, two-dimensional, and includes fully variable properties. Because it uses a single global reaction with integer-order exponents for the reactant concentration terms, the model is ‘tuned’ via the chemical kinetic constants when compared initially to an experiment; when this is done, comparisons of the model to the observed behavior in other experiments are performed. For example, the kinetic parameters for a propanol-air system were first selected [13] to agree with a 1g, 21% oxygen axisymmetric experiment [17]; the use of axisymmetric experiments provides the best basis for comparison because both model and experiment are two-dimensional. The selected kinetic constants were then maintained for comparison to other 1g experiments and with 0g experiments. Agreement on spread character and approximate spread rate was excellent between experiment and model, as shown in Table 1b.

**TABLE 1** Comparison of model and experiment for axisymmetric propanol pool, [13].

	21% $\text{O}_2$		17.5% $\text{O}_2$	
	1g	$\mu\text{g}$	1g	$\mu\text{g}$
Prediction	14 cm/s	16 cm/s	3.8 cm/s (3.5 Hz)	Extinction
Experiment	15	15	3.5 cm/s (3.9 Hz)	Extinction

While the experimentalists were reluctant to quantitatively compare spread rates at the two gravity levels due to the small size of the pool and the rapid spread rates, the modelers were able to do such a comparison using larger diameter pools. Gravity is predicted to affect the uniform flame spread rate just as in the superflash regime.

---

b Note that pre-ignition diffusion occurred at 1g in all cases (experimental and numerical)

## PULSATING FLAME SPREAD

The flame-spread rate is steady in all regimes on **fig. 1**, except in the pulsating spread regime where a regular cycle of fast-slow (also known as ‘jump-crawl’) spread is observed, as shown in **fig. 5** for three pool depths. Many explanations of the cause of pulsating spread have been offered historically[2], and additional diverging explanations offered recently, are discussed below.

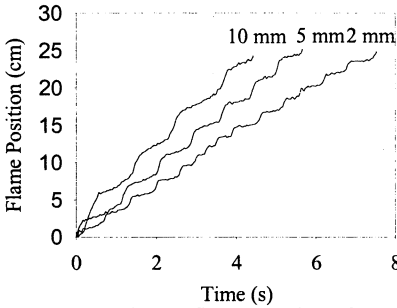


**FIGURE 5** Pulsating flame spread as a function of propanol pool depth in a 2 cm wide x 30 cm long tray, reprinted from [15].

Before examining cause, it is necessary to try to establish the phenomenology of pulsating spread as a function of pool dimensions and gravity level, and detailed diagnostics have provided particular insight in this regard. The following, unless otherwise specified, were accomplished in 1g in pools that were 2 cm wide with a depth of either 10 mm or 25 mm. RSD and PIV measurements were performed to determine the transient flow patterns and temperature fields in the liquid. [20]. Infrared thermography (IR) determined the surface

temperature ahead of the flame. Fuel vapor concentration ahead of the spreading flame was measured via dual wavelength, holographic interferometry [21]. PIV [22] and smoke streamlines [23] visualized gas-phase flow patterns. Flame imaging from the top and side views determined flame shape and position. The combination of these diagnostics yields the following picture of pulsating spread in normal gravity in pools of this size.

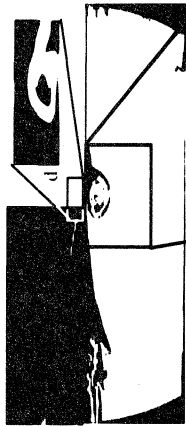
Low-speed flow in the liquid occurs prior to ignition due to evaporation and sedimentation of cold liquid [3]. This renders the liquid pool slightly non-isothermal. Liquid beneath the igniter is heated when the igniter is energized, and a surface flow carrying warm liquid develops away from the igniter. Upon ignition, the flame jumps to near the front of the warm liquid. Viewed from above, the flame front is slightly curved due to losses at the sidewalls (**fig. 6a**), but is symmetric along the tray axis. Viewed from the side (**fig. 6c**), the flame stands off the surface slightly (on the order of a millimeter) due to quenching. The flame then spreads slowly as it enters the crawl phase of the pulsating spread cycle. Rapid interfacial flow in the direction of flame spread develops and precedes the flame front during this phase. The flow drives the formation of a vortex in the liquid that carries warm liquid along the surface ahead of the flame and down into the pool depth (**fig. 6e**). The center of the vortex travels with the crawling flame. Whereas the bottom of the thermal vortex reaches only partway into the depth of the pools, significant convective motion occurs all the way to the bottom of the pool (**fig. 6f,g**). Additional ‘twin vortices’ develop laterally on the surface (**fig. 6b**) due to drag on the sidewalls and the rapid liquid flow along the center of the tray. The combination of these rapidly spinning vortices, existent in the forward and lateral



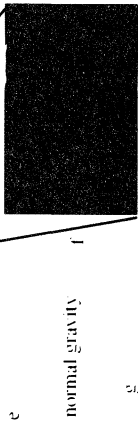
Top view of flame and smoke streak lines.



Top view of liquid surface temperature from IR camera.



Side view of flame and smoke streak visualization of gas-phase recirculation cell.



Side view of liquid-phase temperature gradient field from rainbow schlieren.



Side view of liquid-phase flow in fuel tray via time-lapse particle imaging.

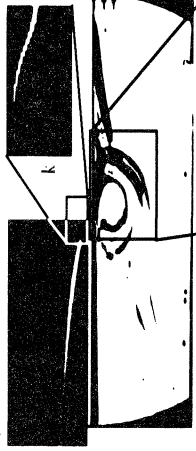
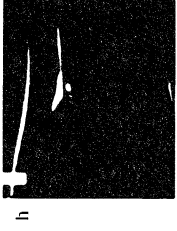


FIGURE 6 Comparison of physical phenomena associated with flame spread in 1g vs.  $\mu$ g. All figures to scale;  $\text{---} = 1 \text{ cm}$ .

directions, renders a complicated temperature and velocity field on the surface. The surface temperature often does not decay monotonically with axial distance ahead of the flame. Between the flame front and the edge of the preheat zone, regions of low temperature on the pool surface are observed, known as surface temperature valleys [20, 21, 24].

At the same time (still in the crawl phase), buoyancy and/or a mechanical fan draws air toward the flame. As visualized by smoke, air traveling close to the surface on a streamline near the sides of the pool are pushed laterally away by thermal expansion near the flame front (fig. 6a). After passing the flame front, the airflow begins to turn back toward the flame again in 1g as it is caught in the buoyantly driven flow. The flow toward the trailing flame serves to raise the reaction rate and elevate the flame temperature to the point that soot is formed.

Air approaching along the surface and directly in front of the center of the flame curls downward to form and grow into the gas recirculation cell (fig. 6d). Smoke in streamlines farther from the surface do not curl under and recirculate, but instead expand laterally around the flame (fig. 6a). Interestingly, the smoke never appears to pass to or through the flame itself. In contrast, the larger particles used in gas-phase PIV did sometimes traverse the flame front, accelerating upon their passage through the front.<sup>c</sup>

Some of the warm liquid on the surface ahead of the flame evaporates and diffuses into the recirculation cell. In the gas above the temperature valleys, the local fuel vapor concentrations are lower than in the neighboring gas [21]. The fuel vapor in the cell accumulates and tends to homogenize until it just reaches a flammable concentration. At this time, the recirculation cell is largest. The flame then jumps forward to a location where the local fuel vapor concentration outside the quench layer is at a concentration corresponding roughly to the lean-limit concentration for a premixed gas system (this is approximately the location on the surface that matches  $T_{FL}$  just before the jump begins). In the process of jumping, the combusting gases thermally expand pushing forward and destroying the recirculation cell. The flame again spreads slowly, and the cycle repeats itself.

An excellent summary schematic of this phenomenology for narrow trays is found in [21]. This phenomenology changes as follows for other geometries. For shallow trays, the tray bottom restricts the sizes of both the main subsurface thermal and convective vortices. This shortens the time of circulation and increases the frequency of pulsation. Additionally, surface deformation [25, 26] due to the rapid interfacial flow becomes very significant for shallow trays. It is to be investigated whether twin vortices develop on the surface of shallow and/or axisymmetric pools. For intermediate depths (say, for trays shallower than about 5

---

<sup>c</sup> One experimental difference should be noted: with the smoke tests, a fan imposed an opposed airflow that maintained the smoke on streamlines parallel to the fuel surface as the flame approached. The smoke was observed to curl around and form the recirculation cell. In the gas PIV experiments, small particles were placed in the air and gradually settled vertically toward the surface, the airflow in this case was buoyantly driven, and the recirculation cell was not observed to form as fully as with an imposed airflow. Smoke-flow tests without an imposed flow also have not revealed a full recirculation cell, but do clearly show airflow toward the flame.



mm), the thermal field reaches the pool bottom, and heat loss occurs. Because there is substantial flow observed in the 10 mm deep tray, it can not be considered to represent the limiting case of a “deep” pool. For pools of 25 mm depth, velocities far below the surface are very small, and this depth can likely be treated as infinitely deep in 1g.

For narrower trays, heat loss to the sidewalls leads to additional flame front curvature but symmetry along the tray’s longitudinal axis is maintained. When the tray is made narrow enough, the sidewalls inhibit the formation of the lateral twin vortices. At the other extreme, wider trays lead to a very erratic flame front shape (discussed below) and irregular spread. Tests have not yet been conducted to adequately describe the temperature and velocity fields in wide trays.

Agreement between predicted and measured spread rate improves when the aspect ratio of width:depth increases [19], as occurs with decreasing depth in a fixed width tray. Comparisons between experiments and models at the next level of detail (e.g. temperature field, surface velocity) are rarely done, and are restricted because models are two-dimensional while most experiments involve three-dimensional phenomena. Given the state of the art in modeling, it might be asked if experiments should be conducted solely in axisymmetric geometries. Experimentalists resist this approach due to the inability to apply detailed diagnostics in such trays.

### **Effects of Gravity Level on Pulsating Spread**

In microgravity, many changes occur which are also functions themselves of pool depth and width. Pulsating flame spread behavior in a *quiescent*, microgravity atmosphere, where buoyant flows in both the liquid and gas phases are negligible, is never observed. Instead, independent of O<sub>2</sub> concentration, fuel or diluent type, and tray geometry, the initial conditions that give rise to pulsating flame spread in 1g coincide with those causing extinguishment in a quiescent,  $\mu$ g environment [17]. Later experiments [16] showed that the flame is sustained in  $\mu$ g with a forced, opposed air flow, where under quiescent  $\mu$ g conditions, it extinguishes. As is the case with solid fuels, a slow, opposed gas-phase flow lowers the limiting oxygen concentration. The authors in [16] observed non-uniform spread across 10 mm deep pools, but could not determine whether the spread was pulsating or merely erratic due to irregularities in the airflow or other experimental features (e.g. liquid sloshing tied to the transition from 1g to  $\mu$ g). Recently, drop tower experiments were conducted again, with special care given to the forced airflow uniformity. Two rectangular trays were used, each being 150 mm long and 2 mm deep, with widths of 80 mm and 20 mm, with flame propagation against a 20-36 cm/s airflow. For the first time, experiments (with the narrower tray) display pulsating spread in  $\mu$ g. Due to the limited drop time, only a few pulsations are seen, but the tests are consistent enough that pulsating spread is verified. Unlike 1g pulsations, the flame retreats before its brightness increases and it surges forward.

With the wider tray, new phenomena are observed. Sample flame fronts from 1g and  $\mu$ g experiments with the wide tray are shown in **fig. 7a,b**. One interesting feature of both the 1g and  $\mu$ g flames is that they no longer have simple curved fronts, but instead exhibit “fingering,” whereby parts of the flame are convex and others concave to the direction of spread. This is unlike the results for pools that are the same depth but are only 20 mm wide,

where flames have a consistently shaped, slightly convex flame front, similar to **fig. 6a,h**.

The fingers in the wide tray are not steady in time, but may retreat and advance in what appears to be an erratic fashion. This highly wrinkled and erratic front makes it difficult to characterize the flames as



**FIGURE 7** Top view of flame spread across an 80 mm wide by 2 mm deep pool of 1-butanol. (a) 1g: Smoke lines indicate flow pattern 1 mm above surface. Free-stream flow is left-to-right at 30 cm/s, while spread is right-to-left. (b)  $\mu\text{g}$ : flame is more erratic in shape, direction, and brightness. Curved bright line on right is a glowing igniter wire.

regularly pulsating, but spread is certainly dissimilar to traditional uniform or pseudo-uniform spread in narrower trays. On a qualitative level, the  $\mu\text{g}$  flames are more unstable (frequency and amplitude of oscillations were larger) than their 1g counterparts, perhaps because of a sloshing liquid pool in  $\mu\text{g}$  due to the drop or due to waves generated by the ignitor or the flame itself, or because of the presence in 1g of a stabilizing buoyant flow in addition to the imposed airflow. This unsteadiness is also manifested in the flame position graphs where the oscillations along the centerline are larger. For each of the pools, the flame position vs. time was determined (**fig. 8**). Perhaps the most unexpected feature of the flame spread is that it is as fast or *faster* in  $\mu\text{g}$  than in 1g for the same opposed airflow rate. In no previous tray geometry has this been found.

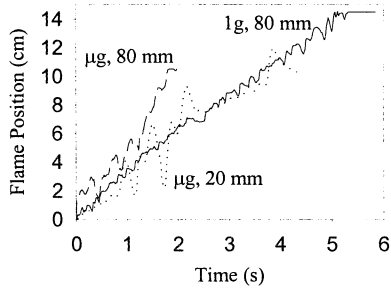


**FIGURE 8** Flame spread across butanol pools of 2 mm depth in an opposed 30 cm/s airflow.

When deeper (rather than wider) pools were examined in  $\mu\text{g}$  experiments, new behavior once again was discovered[20]. Slow, quasi-steady spread of an entirely blue flame was observed, rather than the expected pulsating spread. The slow  $\mu\text{g}$  flame velocity, observed at all forced air speeds, is an order of magnitude less than that which occurs on earth in the uniform spread regime. This behavior, supported by detailed RSD and PIV measurements, suggests the flame spread character is unrelated to classically defined uniform spread. Instead, the authors speculated that it is similar in magnitude and character to the slow spread velocity associated in 1g with the crawling phase of the pulsation cycle or the pseudo-uniform spread regime. Ito et al [21] later confirmed this conclusively in 1g experiments.

The differences in the flow and temperature fields between 1g and  $\mu$ g are shown on **fig. 6**, and are described in detail in [20, 23, 27]. In general the liquid vortices (thermal and velocity) are larger and extend further into the pool depth and ahead of the flame. Similarly there is a larger gas-phase recirculation cell (**fig. 6k**). In  $\mu$ g the air ahead of the flame experiences lateral thermal expansion that appears similar to the upstream expansion in 1g (**fig. 6a, h**).

## SUBFLASH, PSEUDO-UNIFORM SPREAD

The nature of this regime is slow, quasi-steady flame spread, similar to the speeds seen in the crawling phase of the pulsating regime. Its name derives from Akita [8] who suspected that the flame would pulsate in a long enough tray, but that pulsations were not observed because the natural pulsation wavelength is longer than the experimental trays that he used. In subsequent experiments in longer trays, flames spreading appear to retain their slow, steady character. Infrared thermographs of the liquid surface [21, 28] reveal 3-D behavior with long, asymmetric preheat areas and surface temperature valleys whose temperatures are below  $T_{FL}$ .

Despite the 3-D behavior, this regime is considered more amenable to a range of models because the flame spread rate is quasi-steady. Assuming boundary layer behavior and a given preheat distance, a similarity solution of the liquid phase [28] predicts that the local surface temperature difference,  $T_s - T_o$ , varies with the square root of distance ahead of the flame. This prediction, which did not include buoyancy effects, was best verified in 1g tests with low viscosity alcohols and trays wide enough to minimize 3-D effects in the liquid while narrow enough to minimize 3-D effects in the gas [28]; independent  $\mu$ g experiments naturally absent of buoyancy provided further proof [20]. These findings imply that buoyant stratification, which affects the driving potential for thermocapillary flow, does not apparently affect the square root dependence of  $(T_s - T_o)$  on preheat distance. Very near the flame front, the boundary layer assumption is admittedly not valid [28, 29] and the surface temperature rises sharply. The liquid phase therefore requires more detailed modeling, which was accomplished through a multiple scaling and full numerical approach [30]. None of the aforementioned models, however, consider the gas phase. When the gas phase was included, pulsating rather than pseudo-uniform spread behavior was predicted in the model of [19], until recently when improved chemical kinetic constants were used [Kim, personal communication]. The model predicts as seen in experiments that the flame spread is really quasi-steady, with a slight acceleration usually present. The acceleration may be due to the length of the tray as compared to the length over which significant surface flow is seen ahead of the flame (known as the flow head, in [19]). If the tray length is small relative to the flow head, the flow and heat transport ahead of the flame is restricted, and the recirculation rate in the liquid increases, causing the flame to accelerate.

## SOME REMAINING QUESTIONS

There are many questions that this review and its predecessor [2] raise, and herein we will attempt to discuss only a few.

## **What role does buoyancy play in driving the liquid-phase flow in the subflash regime?**

There has been considerable debate regarding the importance of the driving forces to surface flow. The forces are inherently coupled with time-dependent magnitudes. For example, if thermocapillarity is small, heating of the pool will occur via conduction farther into the pool depth, which will in turn drive buoyant flow. On the other hand, buoyancy can stabilize the warm liquid near the pool surface and restrict the main liquid vortex to be near the liquid surface; this affects both the vortex recirculation rate and the surface temperature profile that then governs the thermocapillary-driven flow.

The thinness of the subsurface heated layer, combined with the fast rate of spread, makes it unlikely that buoyancy drives the flow in the uniform spread regime. In the pulsating regime, there can be more debate. A series of 1g experiments varied pool depth to examine if buoyancy in the liquid phase might be important in pulsating spread [16]. The experiments showed that the average flame propagation rate and pulsation wavelength increased monotonically over the range of depths from 2 to 10 mm (fig. 5), but the power-law dependence of the average flame spread rate on depth implies that surface tension is the primary driving mechanism in the liquid flow [16]. Numerical models of flame spread also consistently predict that thermocapillary forces dominate buoyancy in the liquid phase [19, 25, 31] under these conditions. According to the numerical model, liquid-phase buoyancy can affect the flow pattern in the liquid but has little effect on the mean or instantaneous flame spread rate [19] for the tested conditions. This conclusion was reached by comparing full 1g and  $\mu\text{g}$  simulations of pulsating flame spread across 10 mm deep pools of n-propanol with buoyancy artificially eliminated in either (a) the liquid phase or (b) the gas phase. The results are sensitive to the gravity level in the gas phase but vary little with the gravity level in the liquid phase.

Recent results show, however, that this conclusion may need modification when deeper, colder pools are involved [32]. Just as decreasing pool depth was shown to change spread from uniform to pulsating in high temperature experiments [16], an increase in pool depth is predicted to change the spread character from pulsating to pseudo-uniform when a pool of propanol is made sufficiently cold and flame spread is slow. As was speculated in [2, 20], buoyant stratification in the liquid becomes important especially in very slow flame propagation involving deep pools. The slower the flame spread rate, the more time is available for stratification of warm liquid to occur, thus buoyancy can have increased importance for pools with  $T_o \ll T_{FL}$  (verified further in [33]). Therefore, while buoyancy does not directly drive the surface flow in pulsating spread, buoyant stratification affects the rates of surface flow and flame spread.

**Why does pulsating flame spread occur for shallow pools but not for deep pools, in microgravity, while pools of either depth pulsate in normal gravity? Why does the model not predict this behavior? Why does the  $\mu\text{g}$  flame spread pseudo-uniformly but the 1g flame pulsates when the pool depth is large?**

The first thought is that the absence of buoyant stratification causes the flame spread to be slow in  $\mu\text{g}$ , so slow that the spread character for deep pools is altered. The numerical model [19] accounts for buoyant stratification, however, and it was predicted that, at either depth

used in the experiments, pulsating spread would occur in  $\mu\text{g}$  with the imposed opposed airflow. It was therefore concluded that some other mechanism, unaccounted in the model, was causing the change in spread character. To initially try to explain this disagreement, dimensional effects were examined[20]. The model is two-dimensional and cannot account for the effects of a finite flame width or the sidewall losses associated with the tray (whose width:depth aspect ratio was 0.8). One consequence of this difference is that hot gas expansion in the model is inherently constrained to the vertical and longitudinal directions. In general, however, hot gas expansion can occur in these directions and also in the transverse direction. Hence gas expansion toward the sides – a mechanism available in the experiments but not in the model – could decrease the extent of hot gas expansion ahead of the flame. It was decided therefore to artificially reduce the gas thermal expansion in the model. When this was done, satisfactory agreement could be obtained between the predicted and observed spread rates and the steadiness of the spread[20, 34]. When this same artificiality was introduced into the 1g model, however, the predicted flame spread character also changed to pseudo-uniform, which disagreed with the 1g experiments where the spread is pulsating.

It was then speculated that gas-phase buoyant flow might oppose the lateral gas expansion in the 1g experiment, so that the 1g flame retained its pulsating character. If so, it was anticipated that greater flow divergence caused by lateral expansion would be measured in  $\mu\text{g}$  in the absence of a buoyant flow directed towards the flame. Recent results, however, suggest that the thermal expansion ahead of the flame in  $\mu\text{g}$  is not dramatically different than in 1g (fig. 6 a,h), except that the smoke traces near the trailing  $\mu\text{g}$  flame do not rise nor turn inward in the absence of buoyancy, unlike those displayed in [23]<sup>d</sup>.

Thus, alternative reasons are still needed to explain the observed behavior. Radiative heat loss is not yet in the model. This kind of loss weakens  $\mu\text{g}$  flames proportionately more than 1g flames in experiments with solid fuels[35, 36]. There is every expectation that the same behavior will be predicted in flame spread across liquid fuels. It is known from the flame luminosity in experiments that the  $\mu\text{g}$  flames are weaker than in 1g, perhaps due to radiative heat loss. If so, the accounting for radiative loss in the model may enable the prediction of pseudo-uniform spread as is observed in  $\mu\text{g}$  while retaining the pulsating character of spread found in 1g. If this is the sole cause, however, then why do shallow pools in  $\mu\text{g}$  pulsate when these would still be experiencing radiative loss? With shallow pools, though, heat loss and stratification into the pool depth are absent and the flame pulsates at a higher frequency and is generally more robust, making it less susceptible to radiative loss.

### **What causes pulsating spread?**

All of the historical reasons offered as the cause for pulsating spread are now disproved (a review of them can be found in [2]), and have been replaced by the following theories:

---

<sup>d</sup> The absence of this side flow phenomenon likely suppresses soot formation in the  $\mu\text{g}$  experiments, resulting in the all-blue flames during spread even at the relatively high forced air speeds. After spreading across the whole pool, the pool temperature rises, increasing the evaporation and reaction rates, so that soot is eventually produced in the trailing flame.

- a. A cyclic formation and destruction of a gas-phase recirculation cell must occur for pulsating spread to exist [19].
- b. The steep velocity gradient in the liquid just under the flame causes the flame position to move suddenly if the gradient is perturbed [30]
- c. Just as in premixed gas systems, the high Lewis number of the fuel vapor-air mixtures provide a sufficient imbalance in heat and mass transport rates to yield oscillatory behavior [37]
- d. The existence of surface temperature valleys delays spread until fuel vapor accumulates to a sufficient level in the recirculation cell and then the flame jumps [21]

Each of these is discussed briefly. Note that a and d require both phases to participate, while b only relies on the liquid, and c only on the gas. A key criterion in evaluating each of these theories is that they should be able to predict the onset of pulsating spread both from the low-temperature side and from the high-temperature side, because pulsating spread occurs only over a small range of temperatures. Table 2 shows various means to achieve transitions to and from pulsating spread.

**TABLE 2**

<b>Means to Effect Transition</b>	<b>Uniform <math>\Rightarrow</math> Pulsating</b>	<b>Pulsating <math>\Rightarrow</math> Pseudo-Uniform</b>
Lower pool temperature	Predicted and shown by 1g experiments	Predicted and shown by 1g experiments
Changed pool depth	Predicted in 1g and $\mu$ g with forced airflow. 1g experiments without forced flow show decreases in pool depth can cause this transition	Predicted that increases in pool depth can cause this transition; not yet examined in expts.
Reduced lateral gas expansion	Not yet examined in 1g or $\mu$ g	Predicted; no direct test, however, enhanced lateral gas expansion was not seen in $\mu$ g experiments
Lower oxygen concentration	Predicted and shown by expts in 1g; predicted and shown by expts to go from Uniform $\Rightarrow$ Extinction in quiescent $\mu$ g. Not examined with forced gas flow.	Predicted not to occur at any g level; not yet examined in 1g or $\mu$ g expts.
Reduced gravity	Not found for case with forced gas-flow; in quiescent $\mu$ g, transition to flame extinction, rather than pulsating spread, is observed & predicted	Predicted not to occur, but observed in $\mu$ g experiments with forced airflow
High diffusivity diluents	Found in 1g and $\mu$ g experiments with He/O <sub>2</sub> ; superflash spread, however, is predicted.	Not yet examined
Increased opposed airflow velocity	Predicted in 1g. Not yet examined in expts.	Not yet examined
Decreased surface-tension coefficient?	Not yet examined	Not yet examined
Radiative heat loss?	Not yet examined	Not yet examined

As noted in [19], the onset of pulsating spread correlates with the formation of the gas-phase recirculation cell, not with the existence of liquid-phase convection ahead of the flame as once thought [24]. At higher temperatures, the flame spread rate outpaces the formation of the recirculation cell, and the flame spreads uniformly. At low temperatures, the recirculation

cell becomes sufficiently large that it never accumulates fuel vapor in sufficient concentration outside the quench layer to jump forward [21]. The parametric studies in [19] show the flame spread character and rates are strongly affected by fuel volatility and chemical kinetic constants and affected less strongly by the liquid viscosity and the surface-tension temperature coefficient. All of these parameters affect the transition value of the initial pool temperature leading to flame pulsations but do not change the dependence of flame pulsations on the existence of the gas-phase recirculation cell. In particular support of this theory are experiments in quiescent  $\mu\text{g}$  [17], or in 1g with high-speed concurrent air flow [27], where no recirculation cell should exist, and pulsating spread is not observed. Other means, such as a decreased surface-tension coefficient, liquid-flow restrictions or an increased opposed airflow velocity, may also limit the formation of the recirculation cell, but these are yet to be examined.

As noted in [30], pulsating flame spread has been predicted based solely on thermocapillary-driven liquid-phase phenomena (no buoyancy effects, no gas-phase effects). The flame position is taken as that where  $T_{\text{FL}}$  occurs. For selected distributions of heat flux from the flame to the liquid surface (as must be estimated from means outside the model), the flame position moves forward in a pulsating manner. The reason the flame position pulsates is that the thermocapillary-driven flow induces a very steep longitudinal velocity gradient. Small perturbations to these gradients will rapidly change the flame position. Once a new position is found, time is required for a new gradient to be established. Once established, the cycle repeats itself. With heat fluxes outside the selected range (as might occur at sufficiently high or low  $T_0$ ), steady spread is predicted. No comparison has yet been done quantitatively with experiments. For comparison, accurate measurement and prescription of the transient heat flux distribution incident on the pool surface are required; this is not easily accomplished experimentally.

It has recently been theorized [37] that the same phenomena that causes near-extinction oscillations in  $\mu\text{g}$  candle flames and other edge flames may be responsible for pulsating spread. The oscillations are interpreted as an instability that is a combination of large Lewis number ( $Le \approx 2-3$ ) and heat losses from the front-most edge of the flame. It is noted that the trailing diffusion flame does not oscillate, so phenomena near the flame front should be controlling the pulsating process. Based on this model, oscillations of the flame front position have been predicted. Again, no buoyant mechanism is required, nor are any liquid-phase phenomena. No detailed comparisons have been made yet with experiments. While it is debatable as to whether it applies to some aspects of pulsating spread, this mechanism may explain the erratic flame behavior observed with wide pools, and those observed in helium-diluted environments described in [17]. Helium dilution produces a new type of spread in 1g across the pools of light alcohols: spread in 1g becomes highly oscillatory at all initial temperatures, at frequencies that, due to the inherently slow response of the pool, appears unconnected with any liquid-phase phenomena.

Finally, the hypothesis of [21] seems connected with that of [19]. With surface temperature valleys, the local fuel vapor concentration is below that of the neighboring gas. If that local concentration is below a flammable level, then the flame front can not advance through this region, and flame spread will be delayed (the crawl portion of the pulsating cycle). With time, diffusion and convection in the recirculation cell will transport higher concentration

vapor into regions of low concentration, and the flame will spread rapidly through it. The reasons cited above for the high and low temperature limits of pulsating spread apply here as well. It remains to be proven whether the existence of a temperature valley is required for pulsating spread.

Independent of any of these theories, it seems logical [16] that pulsating spread is affected both by liquid-phase transport (as seen by the experimental correlation with the requirement for liquid-phase convection preceding the flame for some of the pulsating cycle) and by gas-phase transport (as seen by the correspondence with a gas recirculation cell, and the effects of oxygen concentration, diluent type, air-flow direction and speed).

**Is the flame response to forced airflow and buoyant airflow qualitatively and quantitatively similar, for liquid pools? Why is a higher opposed airflow speed required to sustain a  $\mu\text{g}$  flame spreading across a liquid pool than is required for a solid fuel plate?**

It is easily observed that flame shapes are different in the trailing portions of buoyant flames as compared to  $\mu\text{g}$  flames in a forced airflow. Because flame spread across solid fuels is controlled by phenomena at the leading edge and the velocity profiles in this region are approximately alike, similar flame spread behavior is predicted when buoyant airflow is replaced by forced airflow in the direction that opposes downward flame spread [38a]. Buoyant and forced gas flow fields can also be made effectively identical through proper transformation [38b] for solid fuels burning in stagnation point geometries. Finally, low-speed forced airflow sustains flame spread in  $\mu\text{g}$  because the forced airflow replaces buoyant flow of oxidizer toward the flame front. While all this is true for solids, flame spread across liquid pools is not as simple due to surface motion, the presence of the gas-phase recirculation cell, and the larger pools used in experiments. For example, the buoyant velocity just ahead of the leading edge of the liquid pool flame (at the flame front) is predicted to be about 5-10 cm/s [19] with a sharp acceleration behind the flame<sup>e</sup>. With a forced freestream speed of 5 cm/s replacing buoyant airflow, however, extinction is observed in  $\mu\text{g}$  experiments with room-temperature butanol pools [27]. At higher freestream speeds, when the velocity at the flame height may be closer to 5-10 cm/s, the flame is sustained.

Interestingly,  $\mu\text{g}$  flame spread across thin [40, 41] and even thick solid fuel plates is sustained with opposed freestream air speeds at 5 cm/s, and often much less than this value. Given much larger radiative losses from the solid surface and the higher pyrolysis temperatures of solids, one might expect that a higher, not lower, forced air speed would be required to sustain flame spread across solids in  $\mu\text{g}$ . This might be explained as follows. For either solid or liquid fuel, a boundary layer builds up with forced airflow, and unless the flame changes its height above the surface (experimentally it does not appear to change), it propagates against airflow of varying speed. At the location of the igniter, the much longer liquid pools have a thicker boundary layer than the short solid fuel plates. The liquid pool flame therefore

---

<sup>e</sup> Scaling estimates place it at somewhat larger values (about 20 cm/s in [39]). To date, a detailed comparison of the predicted 1g, buoyant flow field to the  $\mu\text{g}$ , imposed flow field has not been done. Experimental efforts to measure the buoyant velocities in 1g with smoke traces yield horizontal velocities of about 15-20 cm/s as the flame approaches.



may be trying to establish and propagate against a lower velocity and different velocity gradient. Therefore, the freestream velocity alone is not enough to characterize the local flow condition encountered by a spreading flame.

For either system, buoyant airflow can be enhanced or counteracted by an imposed wind (e.g. via a fan or blow-down system). The natures of flame spread and the resulting convective fields for low-speed *concurrent* airflow, alone or in mixed convection, are completely unstudied for superflash and pseudo-uniform pools, but have been considered in the pulsating regime [27].

## CONCLUDING REMARKS

While much has been learned about the phenomena of flame spread across liquid pools, it should be obvious from the above review that much remains to be done. Only recently have flame spread in the pseudo-uniform and the superflash regimes been examined in earnest. The array of diagnostic instrumentation brought to bear for the past decade on subflash pools now needs to be applied to superflash pools. Hypothesized explanations for observed flame spread behavior in  $\mu\text{g}$  need closer examination. Predictions do not yet account for tray width effects, so direct comparisons with experiments are often impossible. Predicted behavior is dependent on a number of highly sensitive input variables (e.g. chemical kinetic parameters). Flame spread modeling therefore must be extended to three spatial dimensions, and account for physical processes that are likely to be important, including surface deformation, radiative heat loss, and more accurate chemical reaction kinetics. Measurements of these important phenomena also need to be accomplished.

As with most fundamental combustion research, there appears to be a quasi-equilibrium between the number of newly gained insights and the number of remaining questions in flame spread across liquid pools.

## REFERENCES

1. Linan, A. and Williams, F. A., *Fundamental Aspects of Combustion*. 1993, New York: Oxford University Press.
2. Ross, H. D., *Prog. Energy Combust. Sci.* 1994, **20**: p. 17-63.
3. Miller, F. J. and Ross, H. D., in 8th International Symposium on Transport Processes in Combustion. 1995: San Francisco, CA, pp.736-744.
4. Sirignano, W. A. and Schiller, D. N., in *Physical Aspects of Combustion, a Tribute to Irvin Glassman*, Dryer, F. L. and Sawyer, R. F., Ed., 1997, Gordon and Breach. pp. 353-407.
5. T'ien, J. S., Fernandez-Pello, A. C., Ross, H. D., and Miller, F. J., in *Fire in Free Fall*, Ross, H. D., Editor. 2000, Academic Press (to be published).
6. Miller, F. J., White, E. and Ross, H. D., 1994, NASA CP 10194, pp. 343-349.
7. Phillips, H. in Tenth Symposium (Intl.) on Combustion. 1965, The Combustion Institute, pp. 1277-1284.
8. Akita, K., in 14th Symposium (Intl.) on Combustion, 1973, The Combustion Institute, pp. 1075-1083.
- 9a. Feng, C.C., Lam, S.H. and Glassman, I., *Comb. Sci. Tech.*, 1975, **10**: p. 59-71.

- 9b. Kaptein, M. and Hermance, C. E., in 16th Symposium (Intl.) on Combustion, 1976, The Combustion Institute, pp. 1295-1305.
10. Hirano, T., et al., Comb. Sci. Tech., 1980. 22: p. 83-91.
11. White, E.B., *Flame Propagation Through Fuel Vapor Concentration Gradients*, 1997, MS. Thesis, Case Western Reserve University.
12. Miller, F.J., Easton, J., Ross, H. D., and Marchese, A. in NASA/CP-1999-208917.
13. Kim, I., Schiller, D. N., and Sirignano, W. A., Combust. Sci. Tech. 1999, to appear.
14. Matsumoto, Y. and Saito, T., Trans. JSME, Series B (in Japanese), 1980. 46: pp. 998.
15. Ito, A., Masuda, D. and Saito, K., Combustion and Flame, 1991. 83: pp. 375-389.
16. Miller, F.J. and Ross, H. D., in 24th Symposium (Intl.) on Combustion, 1993, The Combustion Institute, pp. 1703-1711.
17. Ross, H. D. and Sotos, R.G., in 23rd Symposium (Intl.) on Combustion. 1991, The Combustion Institute, pp. 1649-1655.
18. Miller, F.J., Ross, H. D. and D.N. Schiller, in *1994 Fall Technical Meeting The Eastern States Section*. 1994, Combustion Institute: Pittsburgh, PA.
19. Schiller, D. N., Ross, H. D. and Sirignano, W. A., Combust. Sci. Tech., 1997. 118: 203-255.
20. Ross, H. D. and Miller, F. J. in 26th Symposium (Intl.) on Combustion. 1996, Combustion Institute, pp. 1327-1334.
21. Ito, A., Konoshi, T., Narumi, A., Tashtoush, G., Saito, K., and Cramers, C. J., in *5th ASME/JSME Thermal Engineering Joint Conference*. 1999. San Diego, CA.
22. Ito, A., Narumi, A., Konoshi, T., Tashtoush, G., Saito, K., and Cramers, C. J., ASME Heat Transfer Division, 1997. HTD-Vol. 352: pp. 141-148.
23. Miller, F. J. and Ross, H. D., in 27th Intl. Symposium on Combustion. 1998, The Combustion Institute, pp. 2715-2722.
24. Glassman, I. and Dryer, F. L., Fire Safety Journal, 1981. 3: p. 123-138.
25. Torrance, K. and Mahajan. R. L., Combust. Sci. Tech., 1975, 10, 125.
26. Hsieh, K.-C. and Pline, A. D., AIAA-91-1306, 1991. AIAA 26th Thermophysics Conference (June 24-26, 1991): Honolulu, Hawaii.
27. Ross, H. D. and Miller. F.J., in 27th Intl. Symposium on Combustion. 1998. The Combustion Institute, pp. 2723-2730.
28. Garcia-Ybarra, P.L. et al, in 26th Intl Symposium on Combustion. 1996, The Combustion Institute, pp. 1469-1475.
29. Sharma, O. P. and Sirignano, W. A. AIAA-71-207, 1971.
30. Higuera, F.J. and Garcia-Ybarra, P. L., Combust.Theory Modeling, 1998, 2, 43-56.
31. Torrance, K.E., Combust. Sci. Tech., 1971. 3: 133-143.
32. Ross, H. D., and Miller, F. J. in NASA/CP-1999-208917.
33. Kuwana, K., Suzuki, M., Dobashi, R., and Hirano, T. in Fire Safety Science -- Proceedings of the Fifth Intl. Symposium, 1997, Melbourne, Australia, pp. 367-378.
34. Ross, H. D., Miller, F. J. and Sirignano, W. A. 1997, NASA CP 10194, p. 375-381.
35. Olson, S. L., Ferkul, P. V. and T'ien, J. S., 22nd Symposium (Intl) on Combustion. 1988, The Combustion Institute, pp. 1213-1222.
36. Altenkirch, R. A., et al., AIAA/IKI Microgravity Science Symposium Proceedings. 1991, Moscow, USSR, May 13-17, 1991, ISBN-1-56347-001-2, pp. 305-316.
37. Buckmaster, J. and Zhang, Y., in NASA/CP-1999-208917.
- 38a. West et al, Combust. Sci. Tech., 1992, 83: 233-244.
- 38b. Foutch, D.W. and T'ien, J. S., AIAA J., Vol. 25, Number 7, July 1987, pp. 972-976.
39. Sacksteder, K. R. and T'ien, J. S., in 25th Symposium (Intl) on Combustion, 1994, The Combustion Institute, pp. 1685-1692.
40. Olson, S. L., Combust. Sci. Tech., 1990, 76: 233-249.
41. Kashiwagi, T., et al., 1997, NASA CP 10194, pp. 411-416.